Available online at www.sciencedirect.com
ScienceDirect
J. Biochem. Biophys. Methods 70 (2008) 830–837
JOURNAL OF biochemical and biophysical methods
www.elsevier.com/locate/jbbm

Immobilization of horseradish peroxidase on chitosan/silica sol–gel hybrid membranes for the preparation of hydrogen peroxide biosensor

Wenjuan Li, Ruo Yuan *, Yaqin Chai, Lu Zhou, Shihong Chen, Na Li

Chongqing Key Laboratory of Analytical Chemistry, College of Chemistry and Chemical Engineering, Southwest University, Chongqing 400715, China

Received 10 June 2007; accepted 19 November 2007

Abstract

A simple and effective strategy for fabrication of hydrogen peroxide (H_2O_2) biosensor has been developed by entrapping horseradish peroxidase (HRP) in chitosan/silica sol–gel hybrid membranes (CSHMs) doped with potassium ferricyanide ($K_3Fe(CN)_6$) and gold nanoparticles (GNPs) on platinum electrode surface. The hybrid membranes are prepared by cross-linking chitosan (CS) with 3-aminopropyltriethoxysilane (APTES), while the presence of GNPs improved the conductivity of CSHMs, and the $Fe(CN)_6^{3-/4-}$ was used as a mediator to transfer electrons between the electrode and HRP due to its excellent electrochemistry activity. UV–Vis absorption spectroscopy was employed to characterize the different components in the CSHMs and their interaction. The parameters influencing the performance of the resulting biosensor were optimized and the characteristic of the resulting biosensor was characterized by cyclic voltammetry and chronoamperometry. Linear calibration for hydrogen peroxide was obtained in the range of 3.5×10^{-6} to 1.4×10^{-3} M under the optimized conditions with the detection limit (S/N = 3) of 8.0×10^{-7} M. The apparent Michaelis–Menten constant of the enzyme electrode was 0.93 mM. The enzyme electrode retained about 78% of its response sensitivity after 30 days. The system was applied for the determination of the samples, and the results obtained were satisfactory.

Keywords: Hydrogen peroxide biosensor; Chitosan/silica sol–gel hybrid membranes; Gold nanoparticles

1. Introduction

The rapid, accurate and reliable analysis of H_2O_2 is of great importance in chemical, biological, clinical and many other fields. Numerous methods have been developed for this purpose, including titrimetry [1], spectrophotometry [2], fluorescence [3], chemiluminescence [4] and electrochemistry [5–7]. Among the techniques mentioned above, electrochemistry, has received tremendous attention due to its high sensitivity and high selectivity of peroxidase. The most common electrochemical technique investigated is via the anodic oxidation of H_2O_2 at a metal electrode [8], metal-dispersed carbon paste electrodes [9], platinized sputtered glassy carbon electrode [10], screen printed carbon electrode [11], indium–tin oxide electrode [12]. However, a main problem occurs from the high overpotential and subsequent interference from many other electroactive species. To eliminate this disadvantage, the amperometric analysis coupling peroxidase with a variety of different redox-mediators, such as hexacyanoferrates [13], ferrocene and its derivatives [14,15], quinone [16] and redox dyes [17–19], is one of the most efficient alternative. Therein, $K_3Fe(CN)_6$, the most widely used as inorganic electron mediators, has been used extensively in biosensor because of its excellent electron transferability and a high degree of reversibility. However, analytes are usually detected using $K_3Fe(CN)_6$ in the detection solution, in which the reference, counter electrodes and the sample solution may be polluted, so it would be preferable to immobilize $K_3Fe(CN)_6$ on the electrode surface, which can provide several advantages such as reducing the analytical time and the consumption of the reagent, simplifying experimental design. Moreover, such an electrode could provide a relatively stable response toward a target enzyme without the addition of mediator to the solution. To the best of our knowledge, there are few reports on immobilization of $K_3Fe(CN)_6$ on the electrode surface to prepare biosensor. The reason maybe that the $K_3Fe(CN)_6$, a kind of low

* Corresponding author. Tel.: +86 23 68252277; fax: +86 23 68254000.
E-mail address: yuanruo@swu.edu.cn (R. Yuan).

0165-022X/$ - see front matter © 2007 Elsevier B.V. All rights reserved.
doi:10.1016/j.jprot.2007.11.010

molecular weight soluble mediating species, could diffuse away from the electrode surface into the bulk solution.

Nowdays, many support materials like Nafion, silica sol–gel, chitosan (CS), poly(vinyl alcohol), etc, have been used for co-immobilizing mediator and enzyme, but single material has its own inherent obstacles such as cracking and less biocompatibility. With the development of advanced composite film, more and more attention has been paid to the novel advanced materials to immobilize mediator and enzyme on an electrode surface [20–22]. These hybrid materials can effectively eliminate the brittleness of pure inorganic materials and the swelling property of some pure polymer or hydrogel. Among them, silica/CS, as potential "next generation" membrane materials, has received wide-spread interest owing to their exciting features such as tunable porosity, controllable hydrophobicity and mechanical stability [23]. Therefore, the materials hold much promise in the development of chemical sensors. A number of articles on the application of these materials have appeared. For example, Jaafar Abdullah et al. [24] have stack immobilized a color reagent-MBTH in nafion/sol–gel silicate hybrid film and HRP in chitosan film. Dong et al. [25] have fabricated a new electrogenerated chemiluminescence biosensor by coimmobilization $Ru(bpy)_3^{2+}$ and alcohol dehydrogenase in silica-chitosan composite film, and such modified electrode exhibited much higher response than those obtained at merely chitosan modified electrodes. The feasibility of the specific interaction of the mediators with the composite film provides a promising means for the development of new amperometric sensors. Moreover, due to the possible control over pore size and hydrophobicity, the mediators could be attach specifically to the composite film, which the leaching of the mediators from the composite was avoided [26]. With this idea, 3-Aminopropyltriethoxysilane (APTES), one of the silane-coupling agents, was selected as a cross-linking reagent to cross-link with chitosan to prepare a new chitosan/silica sol–gel hybrid membranes (CSHMs) for the fabrication of biosensor. The resulting CSHMs possess a homogeneous network suited to the encapsulation of a variety of biomacromolecules. In particular, the another key advantage of CSHMs was able to control the porosity and provide rigidity, which is highly suited to immobilizing ferricyanide small molecular. At the same time, negatively charged $Fe(CN)_6^{3-/4-}$ can also be tightly adsorbed within CSHMs containing robust positively charged amino groups by electrostatic interactions. What is more, the composite system could provide a hydrophilic environment that is compatible with the biomolecules, and to efficiently retain the bioactivity of the entrapped enzymes.

To enhance electron transfer between the redox centre of the enzyme and the electrode surface and the poor conductive properties of CSHMs, and hence to increase the sensor sensitivity, many nanotechnology have been exploited in various applications. Gold nanoparticles (GNPs) has gained much more attention in electroanalytical studies because of its unique properties such as easy preparation, good biocompatibility and relatively large surface area [27]. Here, GNPs play dual roles: on the one hand, GNPs could be embedded in matrices through residual amino groups in CSHMs and further provide a natural environment for bimolecular immobilization allowing for longer life stability and retaining their bioactivity. On the other hand, as the merit of GNPs with the high electrical conductivity and electron transfer accelerating capability, the non-conductivity of the CSHMs can be compensated to some extent, which will favor the sensitivity of biosensor.

In the present work, a novel hydrogen peroxide biosensor has been developed by entrapping horseradish peroxidase (HRP) in CSHMs doped with $K_3Fe(CN)_6$ and GNPs on platinum electrode surface. The experiments results indicated that $K_3Fe(CN)_6$ was well protected inside the CSHMs film, thus preventing leaking of the mediator, and further enhance the stability and catalytical activity of immobilized enzyme. UV–Vis absorption spectroscopy was employed to characterize the different components in the CSHMs and their interaction, the parameters influencing the performance of the resulting biosensor were optimized and the characteristic of the resulting biosensor was studied in detail. The proposed biosensor exhibited good analytical performance towards the quantification of hydrogen peroxide.

2. Experimental

2.1. Reagent and materials

HRP (EC1.11.1.7, RZ>3.0, 250 u/mg), APTES, chitosan, chloroauric acid ($HAuCl_4$) and sodium citrate were purchased from Sigma (St. Louis, MO, USA). Hydrogen peroxide (30% w/v) was obtained from Chemical Reagent Company (Chongqing, China). The concentration of the more diluted hydrogen peroxide solutions prepared from 30% hydrogen peroxide was determined by titration with potassium permanganate. Phosphate buffer solutions (PBS) with various pHs were prepared with 0.1 M KH_2PO_4 and 0.1M Na_2HPO_4. The supporting electrolyte was 0.1 M KCl. All other chemicals employed were of analytical grade and used as received. Doubly distilled water was used throughout the experiments. The working solution was deaerated by bubbling N_2 before determination. Gold nanoparticles with mean size of 16 nm were produced by reducing chloroauric acid with sodium citrate at 100°C for half an hour [28,29].

2.2. Apparatus

Electrochemical measurements were carried out on CHI 660A electrochemical workstation (CH Instruments, Chenhua Corp., Shanghai, China). The electrochemical cell contained a three-electrode system where bare or modified platinum disk electrode (2.0 mm in diameter) was used as a working electrode, platinum wire as an auxiliary electrode and a saturated calomel electrode (SCE) as reference electrode. The UV–Vis spectra was performed in the range of 300–750 nm on a type of Lambda 17 UV–Vis 8500 (PE Co., USA) with quartz cuvette (path length 1 cm). The size of GNPs was estimated from transmission electron microscopy (H600, Hitachi Instrument, Japan). All experiments were carried out at room temperature.

2.3. Preparation of CSHMs

Chitosan solution (0.1%) was prepared by dissolving 0.1 g of chitosan in 100 ml of pH 5.0 acetate buffer solution. The

viscous chitosan solution was stirred at 250 rpm for 3 h at room temperature. And then appropriate amounts of APTES as well as HCl were added to initiate the cross-linking reaction. The mixture was stirred at 50°C until homogeneous solution was obtain. The solution was freshly prepared daily just before the fabrication of biosensors.

2.4. Configuration of different modified electrodes

The bare platinum disk electrode (Φ = 2 mm) was polished successively with 0.3 and 0.05 μm Al_2O_3 before modification, rinsed with double-distilled water, and sonicated in acetone and double-distilled water for 5 min, respectively.

10 μl of CSHMs stock solution, 10 μl of HRP solution (2 mg of HRP was dissolved in 1 ml of 0.1 M PBS, pH 7.0), 10 μl of GNPs, and 5 μl 5.0 mM $K_3Fe(CN)_6$ solution were mixed completely in a small beaker. Then 8 μl of the resulting mixture was dropped on the surface of the freshly cleared platinum disk electrode. The electrode was dried at 4°C for overnight, and then the enzyme electrode was immersed in PBS (pH 7.0) for 10 min in order to remove the excess HRP and $Fe(CN)_6^{3-/4-}$ from the electrode surface. Finally, 5 μl of CSHMs was pipetted to cover it and was dried for ca. 6 h at room temperature to obtain modified electrode (CSHMs/HRP-GNPs-$Fe(CN)_6^{3-/4-}$-CSHMs/Pt). The top CSHMs layer can be used as a protection layer to prevent HRP and $K_3Fe(CN)_6$ from leaking in solution. The CSHMs/HRP-$Fe(CN)_6^{3-/4-}$ CSHMs/Pt and CS/HRP-GNPs-$Fe(CN)_6^{3-/4-}$-CS/Pt electrodes were prepared with the same procedures just without the use of GNPs and silica sol–gel, respectively. The prepared electrodes were stored at 4°C in a refrigerator when not in use.

3. Results

3.1. UV–Vis absorption spectra analysis of different components in the CSHMs and their interaction

UV–Vis absorption spectroscopy was used to investigate the interaction among the CSHMs, GNPs and HRP. Fig. 1 displayed the UV–Vis absorption spectra of (a) CS solution, (b) silica sol–gel solution, (c) CSHMs, (d) GNPs, (e) CSHMs mixed with GNPs, and (f) CSHMs mixed with HRP and GNPs. From (a), (b) and (c), we can see, when silica sol–gel was mixed with CS, no major changes was observed. It was a strong indication that the silica sol–gel didn't change its characters in the CS solution. The optical spectrum of GNPs solution (d) has a λ_{max} of 524 nm, which is the characteristic plasmon absorbance of unaggregated GNPs. And when GNPs mixed with CSHMs, there are only several nanometers shift happened in the Soret absorption band area (528 nm for (e)), which suggests that GNPs are uniformly dispersed in the CSHMs and that no obvious aggregation of GNPs occurred [30]. When HRP was added in (e) solution, except the Soret absorption of GNPs demonstrating the stable state of GNPs and interaction between GNPs and HRP, a distinct absorption peak can be observed, which is similar to the absorption of native HRP, indicating that HRP keeps its natural structure and bioactivity in these mixtures.

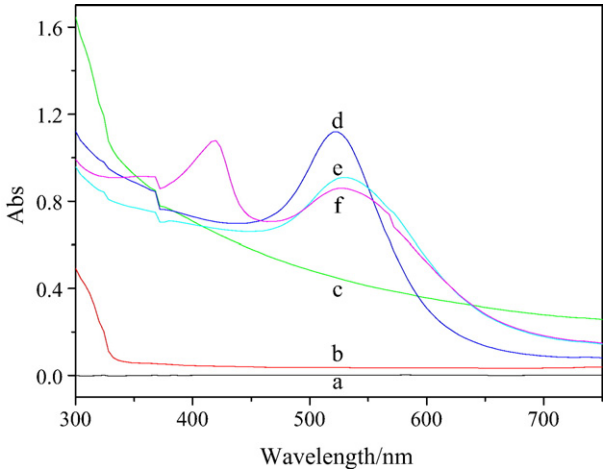

Fig. 1. UV–Vis absorption spectra of (a) chitosan solution, (b) sol–gel solution, (c) CSHMs, (d) gold nanoparticles, (e) CSHMs mixed with gold nanoparticles, and (f) CSHMs mixed with HRP and gold nanoparticles.

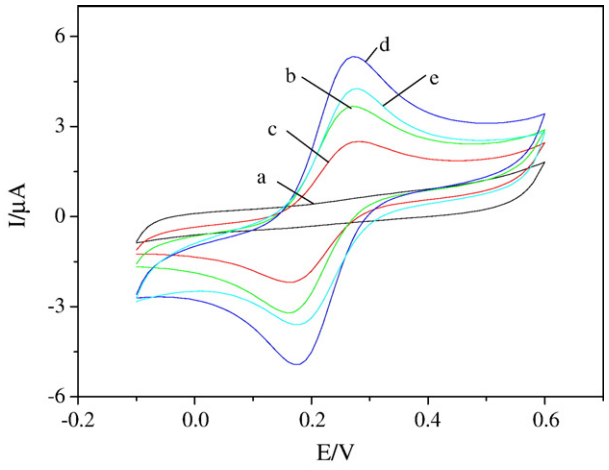

Fig. 2. Cyclic voltammograms (CVs) of CSHMs/Pt (a), CSHMs/$Fe(CN)_6^{3-/4-}$ CSHMs/Pt (b), CS/$Fe(CN)_6^{3-/4-}$ CS/Pt (c), CSHMs/GNPs-$Fe(CN)_6^{3-/4-}$ CSHMs/Pt (d) and CSHMs/HRP-GNPs-$Fe(CN)_6^{3-/4-}$ CSHMs/Pt (e) modified electrodes in 0.1 mol/L PBS (pH 7.0). Potential scan rate, 50 mV/s.

3.2. Electrochemical characterizations

Fig. 2 showed cyclic voltammograms (CVs) of modified electrodes in different composites in 0.1 mol/L PBS (pH 7.0), with a scan rate of 50 mV/s. As can be seen, in Fig. 2 curve a is CSHMs film modified electrode in PBS. We do not find any obvious electrochemical peaks in this potential range as the lack of electron mediator. When $Fe(CN)_6^{3-/4-}$ was adsorbed into CSHMs film via the opposite-charged adsorption technique, the CVs presents a couple of sharp and clear reduction-oxidation peaks of $Fe(CN)_6^{3-/4-}$ (curve b). In contrast, only very weak current was recorded at $Fe(CN)_6^{3-/4-}$ and CS composite film modified Pt electrode (curve c). When the GNPs were assemblied on the electrode, the peak current clearly increase (curve d). After assembling the HRP layer, an obvious decrease of reduction–oxidation peaks were observed (curve e).

With an increasing scan rate the CV peak currents of the CSHMs/HRP-GNPs-$Fe(CN)_6^{3-/4-}$-CSHMs/Pt modified electrode

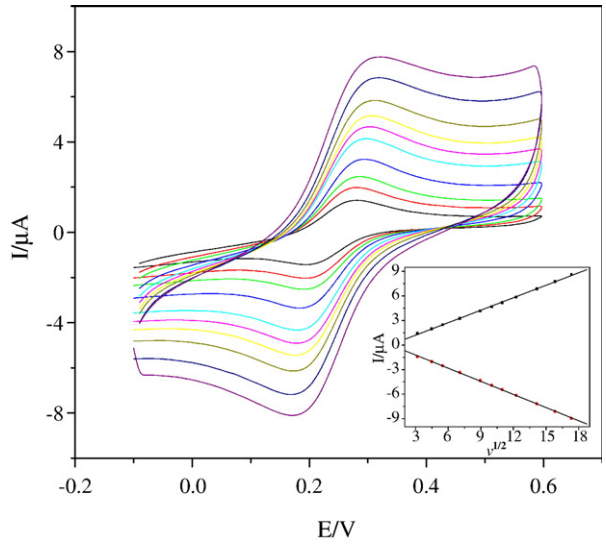

Fig. 3. Cyclic voltammograms of the biosensor at different scan rates (from inner to outer): 10, 20, 30, 50, 80, 100, 150, 200, 250 and 300 mV/s in 5 ml 0.1 mol/L PBS (pH 7.0) under room temperature. Inset: plots of peak currents versus $\nu^{1/2}$.

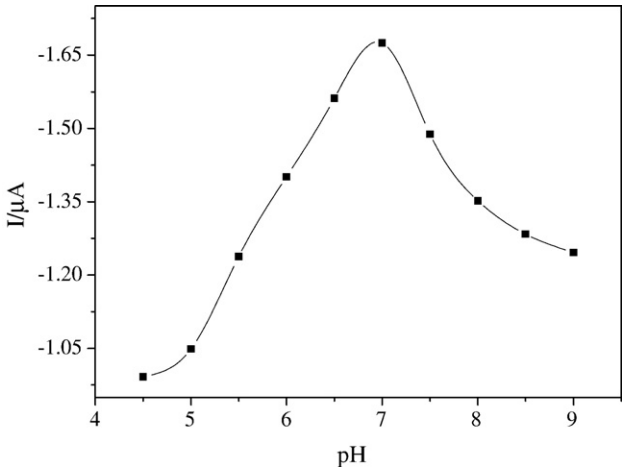

Fig. 5. The influence of pH on the response of the biosensor in 0.1 mol/L PBS containing 0.4 mM H_2O_2.

increased and the peak potentials almost kept at the constant values in the scan rate range of 10–300 mV/s (Fig. 3). The plot of peak current vs. square root of scan rate was shown in the inset of Fig. 3. Which indicates a diffusion-controlled redox process.

Upon addition of 0.14 mM H_2O_2 to electrolyte an obvious electrocatalytic response was observed. The reduction peak current of the CSHMs/HRP-GNPs-Fe(CN)$_6^{3-/4-}$-CSHMs/Pt increased and the oxidation peak current decreased (Fig. 4c and d), indicating a typical electrocatalytic reduction process of H_2O_2. However, no similar cathodic peak corresponding to the reduction of H_2O_2 can be observed at CSHMs/GNP-Fe(CN)$_6^{3-/4-}$-CSHMs/Pt electrode under the same condition (Fig. 4a and b), so it can be concluded that HRP embedded in CSHMs shows good catalytic activity toward H_2O_2.

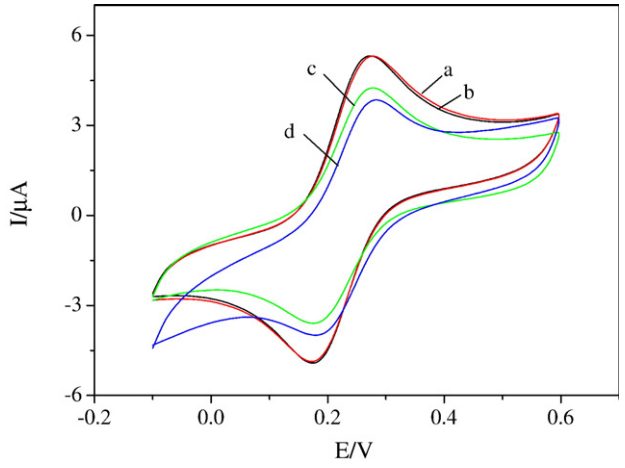

Fig. 4. Cyclic voltammograms of the CSHMs/GNP-Fe(CN)$_6$-CSHMs/Pt and CSHMs/HRP-GNP-Fe(CN)$_6$-CSHMs/Pt electrode without H_2O_2 (a, c), with 0.14 mM H_2O_2 (b, d) at a scan rate of 50 mV/s in 0.1 M PBS (pH 7.0), respectively.

3.3. Influence of pH and applied potential on biosensor response

The pH of the working solution may effect the life time, linear range, detection limit of the biosensor as the immobilized enzyme activity would be effected by the pH of the working solution and the higher or lower pH would destroy the micro-structures of enzyme. The effect of pH was investigated from 4.5 to 9.0. Fig. 5 shows the change of chronoamperometric current with the pH under constant hydrogen peroxide concentration (0.4 mM). As can be seen, the maximum response appears at pH 7.0. To obtain the maximum sensitivity and bioactivity, the PBS of pH 7.0 was used throughout the research.

Fig. 6 shows the dependence of the chronoamperometric current response to constant concentration (0.4 mM) H_2O_2 on the applied potential in the range from −0.2 V to 0.3 V. It can be seen that the response of biosensor increases sharply from 0.3 V to −0.05 V, and reach the maximum at −0.05 V, then decreases at more negative potentials than −0.05 V. Therefore, a constant potential of −0.05 V was adopted in subsequent experiment.

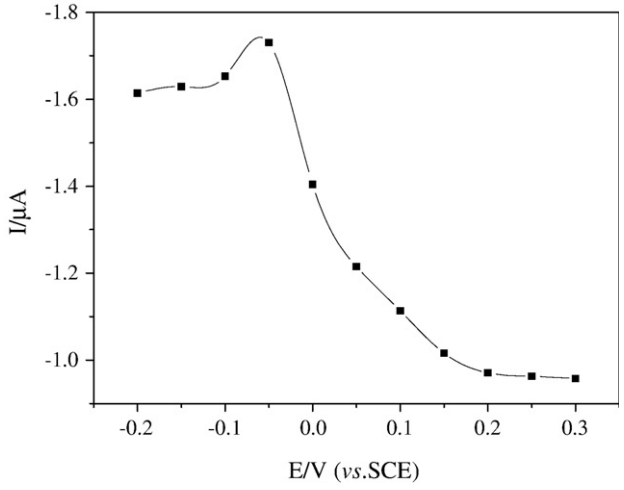

Fig. 6. Dependence of the current response of the biosensor to 0.4 mM H_2O_2 on the applied potential in 0.1 M PBS (pH 7.0).

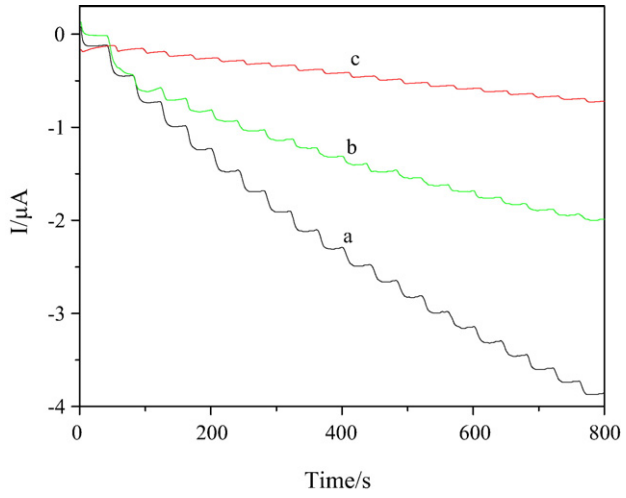

Fig. 7. The chronoamperometry response at applied potential of −0.05 V with injection of 3.5×10^{-4} mol/L H_2O_2 into 5 mL of stirring pH 7.0 PBS for (a) CSHMs/HRP+GNPs+$K_3Fe(CN)_6$+CSHMs/Pt, (b) CSHMs/HRP+$K_3Fe(CN)_6$+CSHMs/Pt and (c) CS/HRP+GNPs+$K_3Fe(CN)_6$+CS/Pt modified electrode, respectively.

3.4. Amperometric response of hydrogen peroxide biosensor

We compared the chronoamperometric response of differently modified electrodes with successive injections of 3.5×10^{-4} mol/L H_2O_2 to 5mL PBS (pH 7.0) at an applied potential of −0.05 V. As shown in Fig. 7, CSHMs/HRP-GNPs-$Fe(CN)_6^{3-/4-}$-CSHMs/Pt electrode (curve a) showed the best response to the addition of the same H_2O_2 concentration. As controlled experiment, CSHMs/HRP-$Fe(CN)_6^{3-/4-}$-CSHMs/Pt electrode (curves b) and CS/HRP-GNPs-$Fe(CN)_6^{3-/4-}$-CS/Pt electrode (curves c) exhibited inferior current responses after the addition of H_2O_2.

The amperometric response of the hydrogen peroxide biosensor was investigated by successively adding H_2O_2 to a continuous stirring 5 mL PBS solution under the optimized conditions. The typical current-time curve of the biosensor is shown in Fig. 8. The response current of the biosensor increases with the increasing of H_2O_2. There is a linear relation of the current with concentration of H_2O_2 between 3.5×10^{-6} and 1.4×10^{-3} M with a correlation coefficient of 0.997 (n = 28), as shown in the inset of Fig. 8. From the slope of calibration curve, the detection limit of 8.0×10^{-7} M is estimated at signal-to-noise rate of three.

The apparent Michaelis–Menten constant K_M^{app} was generally used to evaluate the biological activity of immobilized enzyme and it could be calculated according to the Michaelis–Menten equation [37]: $1/I_{ss} = 1/I_{max} + K_M^{app}/I_{max}C$.

Where, I_{ss} is the steady-state current after the addition of substrate, C referred to the H_2O_2 concentration, and I_{max} is the maximum current measured under saturated substrate conditions and K_M^{app} stands for the apparent Michaelis–Menten constant of the system. K_M^{app} can be obtained by the analysis of the slope and the intercept of the plot of the reciprocals of the steady-state current versus H_2O_2 concentration. The K_M^{app} value for the CSHMs/HRP-GNPs-$Fe(CN)_6^{3-/4-}$-CSHMs/Pt was determined to be 0.93 mM.

3.5. Reproducibility and stability of the hydrogen peroxide biosensor

The stability of the electrode was studied eiectrochemically. When the 100 continuous cyclic scans was carried out with a 50 mV/s scan rate, only 6.8% decrease of the initial response at 0.04 mM H_2O_2 is observed. The relative standard deviation (R.S.D.) is 4.3% for nine successive measurements at 0.04 mM H_2O_2, showing the proposed biosensor possesses a good reproducibility. When not in use, the electrode was suspended above 0.1 M PBS (pH 7.0) at 4°C in a refrigerator. The long-term stability of the proposed biosensor was also studied. The response to 0.04 mM H_2O_2 was tested intermittently. During the first 3 days the response current has about 5.6% decrease and 22% for more than 1 month. Good stability may be attributed to the strong interactions between GNPs and HRP embedded in the CSHMs hybrid film, and large quantities of hydroxyl and amino groups of the CSHMs, which are favorable to maintain the activity of the HRP.

3.6. Interference determination

Six interfering substances (Glucose, Ethanol, Cysteine, Ascorbic acid, L-leucine and L-tyrosine) were used to evaluate the selectivity of the biosensor. The current obtained for each interfering substance at a concentration of 8.0×10^{-4} mol/L in the present of 4.0×10^{-4} mol/L H_2O_2 was recorded and comparing it with the current from the biosensor in the same assay solution containing only 4.0×10^{-4} mol/L H_2O_2. The

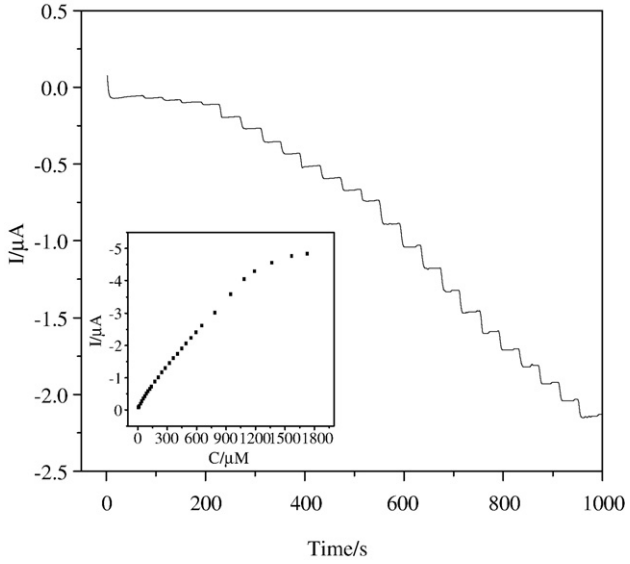

Fig. 8. Amperometric response of the biosensor to H_2O_2 in a pH 7.0 PBS at an applied potential of −0.05 V upon successive additions of 3.50 μM (110–230 s), 10.5 μM (270–390 s), 17.5 μM (430–550 s), 35.0 μM(590–710 s), 42 μM (750–910 s) and 52.5 μM (950–990 s) in the time intervals of 40 s. Inset shows linear calibration curves.

Table 1
Results of interference test

Possible interferents	i_H/i_{H+1}[a]
Glucose	1.022
Cysteine	0.996
L-Leucine	0.982
Ethanol	0.995
Ascorbic acid	0.988
L-Tyrosine	0.998

[a] i_H: response current of H_2O_2 (4.0×10^{-4} mol/L); i_{H+1}: response current of H_2O_2 (4.0×10^{-4} mol/L) in the presence of interferents.

experimental results were listed in Table 1. It is found that the six tested substances did not significantly interfere with the determination of H_2O_2 when the proposed biosensor was employed. This was largely due to the low working potential (about −0.05 V), nearly no electrochemical reactions may occur at this potential.

3.7. Real sample analyses

The feasibility of practical use of the proposed sensor was assessed by testing H_2O_2 concentration in disinfector sample. The sample was diluted 20 times with phosphate buffer solution (pH 7.0). The reference method employed was the classical potassium permanganate titration method. The each assay was tested parallel three times. The calculated results show that the results determined by the HRP electrode were satisfactory and agree closely with those measured by titrimetric method, indicating that it is feasible to apply the proposed H_2O_2 biosensor to determine H_2O_2 in samples.

4. Discussion

This study reported a new method for preparation of hydrogen peroxide biosensor by entrapping horseradish peroxidase (HRP) in CSHMs doped with $K_3Fe(CN)_6$ and GNPs on platinum electrode surface, which would be promising in many fields. The results from Fig. 1 show that the CSHMs GNPs and HRP are well interacted with each others and keep their good states, which is the promising basis for the preparation of our proposed biosensor.

Fig. 2 showed cyclic voltammograms (CVs) of modified electrodes in different composites. A pair of well-defined reduction and oxidation peaks was presented, which demonstrated that $Fe(CN)_6^{3-/4-}$ had the well electroactive performance as an efficient mediator to shuttle electrons. Furthermore, the peak current of CSHMs-$Fe(CN)_6^{3-/4-}$ modified electrodes is larger than of CS-$Fe(CN)_6^{3-/4-}$ modified electrodes, which indicating the CSHMs film can increase the immobilization quantity of $Fe(CN)_6^{3-/4-}$ at the electrode surface. The peak currents increased after immobilizing the GNPs on the electrode. The remarkably increasing current may be explained by the fact that the doped GNPs improved greatly the conductivity of the CSHMs film and the electron shuttle between the mediator and electrode. The reduction–oxidation peaks obvious decrease after assembling the HRP layer, the reason is that HRP acting as the mass transfer blocking layer, hinders the diffusion of the ferricyanide towards the electrode surface. Meanwhile, it also indicated that HRP was immobilized on the modified electrode successfully.

Fig. 3 displayed the dependence of the cyclic voltammogram on scan rate. The finding showed that the biosensor represents well-defined surface waves in cyclic voltammetry, which indicated that the $Fe(CN)_6^{3-/4-}$ adsorbed in CSHMs was efficiently for faciling the charge transfer. As shown in the inset of Fig. 3, the peak currents were proportional to the square roots of the scan rates, indicating that the reduction and oxidation of the enzyme electrode was diffusion-controlled.

In this work, the optimal pH occurred around pH 7.0, which was similar to that of living organisms and HRP can remain more active in neutral solution. Moreover, the low applied potential was favourable to minimize the interference from the coexisting electroactive species.

From Fig. 4, the biosensor showed excellent electrocatalysis for H_2O_2. These results strongly indicated that the catalytic reduction of H_2O_2 originated from the HRP reaction mediated by $Fe(CN)_6^{3-/4-}$. Thus, $Fe(CN)_6^{3-/4-}$ could effectively shuttle electrons from the electrode surface to the redox center of HRP. The reaction mechanism of the biosensor can be summarized as follows:

$$H_2O_2 + 2H^+ + HRP(Red) \rightarrow 2H_2O + HRP(Ox)$$

$$HRP(Ox) + K_4Fe(CN)_6(Red) \rightarrow HRP(Red) + K_3Fe(CN)_6(Ox)$$

$$K_3Fe(CN)_6(Ox) + e^- \rightarrow K_4Fe(CN)_6(Red)$$

Fig. 7. showed the chronoamperometry response of three differently modified electrodes. According to curves a and b, we can see that the GNPs played a very important role on the performance of biosensor, which may be the reason that GNPs can strongly adsorb enzyme and thus prevent the leakage of enzyme. Moreover, GNPs can act as tiny conduction centers which facilitate the transfer of electrons between enzyme and electrode. As for the apparent difference between curve a and c may be explained as follows:

The CSHMs exhibited highly porous structure whereas CS gel was tightly compacted. In contrast to CSHMs, CS gel had a high swelling ratio. Moreover, CS is capable of forming hydrogen bonds with adjacent chains. So when CS gel was dried, it presented severe shrinkage and collapsing structure [31]. These properties of CS gel would reduce the activity and stability of the immobilized enzyme [32].

Thus several dopants were efficiently entrapped in the CSHMs matrix without any restriction to interaction for electron transfer.

Furthermore, the GNPs improved the conductivity of CSHMs matrix and facilitated electron transfer. The K_M^{app} value for the proposed biosensor was 0.93 mM. This K_M^{app} value was smaller than those of 4.8 mM [5] and 4.6 mM [33] for H_2O_2 biosensor based on sol–gel matrix, this suggests that the present sensor exhibits a higher affinity to H_2O_2.

Compared with the similar biosensors [34,35], the linear range of this biosensor was wider under optimal condition. The biosensor owned lower applied potential as compared to that of many reported literatures [35,36], which was favourable to minimize the interference from the coexisting electroactive species. Moreover, the presented biosensor exhibited a relatively fast response and it achieved 95% of response within 10 s, which may be due to the excellent electron transferability and biocompatibility of the mediator. Meanwhile, it also may be attributed to a series of good performances of GNPs. In particular, the proposed biosensing method shows low cost and simplicity, and can be used in the preparation of other amperometric enzyme-biosensors for the detection of important species.

5. Simplified description of the method and its (future) applications

In this experiment, we successed in doping GNPs and Fe $(CN)_6^{3-/4-}$ in CS/silica sol–gel composite, the new complex immobilization matrix integrates the merits of chitosan/silica sol–gel hybrid membranes, GNPs and mediator, and shows excellent conductive, entrapment and biocompatible properties. The composite film was used as model film to construct amperometric hydrogen peroxide biosensors, namely, CSHMs/HRP-GNPs-Fe$(CN)_6^{3-/4-}$ CSHMs/Pt. It exhibits higher sensibility, wider linear range, lower detection limit and better reproducibility and stability. In addition, this biosensor also has strong anti-interference to some potential interfering substances. Such a proposed strategy would be potentially useful for the preparation of other enzyme sensor. The system was applied for the determination of the samples, and the results obtained were satisfactory.

Acknowledgement

This work was supported by the NNSF of China (20675064), the Natural Science Foundation of Chongqing City (CSTC-2004BB4149, 2005BB4100), the Chinese Education Ministry Foundation for excellent young teachers (2002-40) and High Technology Project Foundation of Southwest University (XSGX02), China.

References

[1] Hurdis EC, Romeyn JH. Accuracy of determination of hydrogen peroxide by cerate oxidimetry. Anal Chem 1954;26:320–5.
[2] Matsubara C, Kawamoto N, Takamura K. Oxo[5,10,15,20-tetra (4-pyridyl) porphyrinato] titanium (IV): an ultra-high sensitivity spectrophotometric reagent for hydrogen peroxide. Analyst 1992;117:1781–4.
[3] Zhang LS, Wong GTF. Optimal conditions and sample storage for the determination of H_2O_2 in marine waters by the scopoletin-horseradish peroxidase fluorometric method. Talanta 1999;48:1031–8.
[4] Hanaoka S, Lin JM, Yamada M. Chemiluminescent flow sensor for H_2O_2 based on the decomposition of H_2O_2 catalyzed by cobalt(II)-ethanolamine complex immobilized on resin. Anal Chim Acta 2001;426:57–64.
[5] Li J, Tan SN, Ge HL. Silica sol–gel immobilized amperometric biosensor for hydrogen peroxide. Anal Chim Acta 1996;335:137–45.
[6] Garguilo MG, Huynh N, Proctor A, Michael AC. Amperometric sensors for peroxide, choline, and acetylcholine based on electron transfer between horseradish peroxidase and a redox polymer. Anal Chem 1993;65:523–8.
[7] Xiao Y, Ju HX, Chen HY. A reagentless hydrogen peroxide sensor based on incorporation of horseradish peroxidase in poly(thionine) film on a monolayer modified electrode. Anal Chim Acta 1999;391:299–306.
[8] Guidelli R, Pergolo F, Raspi G. Voltammetric behavior of nitrite ion on platinum in neutral and weakly acidic media. Anal Chem 1972;44:745–55.
[9] Wang J, Naser N, Angnes L, Wu H, Chen L. Metal-dispersed carbon paste electrodes. Anal Chem 1992;64:1285–8.
[10] Zhang Z, Liu H, Deng J. A glucose biosensor based on immobilization of glucose oxidase in electropolymerized o-aminophenol film onplatinized glassy carbon electrode. Anal Chem 1996;68:1632–8.
[11] Wang J, Tian B, Nascimento VB, Angnes L. Performance of screen printed carbon electrode fabricated from different carbon inks. Electrochim Acta 1998;43:3459–65.
[12] Zhang JD, Kambayashi M, Oyama M. Seed mediated growth of gold nanoparticles on indium tin oxide electrodes: electrochemical characterization and evaluation. Electroanalysis 2005;17:408–16.
[13] Schubert F, Saini S, Turner APF. Mediated amperometric enzyme electrode incorporating peroxidase for the determination of hydrogen peroxide in organic solvents. Anal Chim Acta 1991;245:133–8.
[14] Tatsuma T, Okawa Y, Watanabe T. Enzyme monolayer-and bilayer-modified tin oxide electrodes for the determination of hydrogen peroxide and glucose. Anal Chem 1989;61:2352–5.
[15] Mulchandani A, Wang CL, Weetall HH. Amperometric detection of peroxides with poly(anilinomethylferrocene)-modified enzyme electrodes. Anal Chem 1995;67:94–100.
[16] Sanchez PD, Blanco PT, Alvarez JMF, Smyth MR, O'Kennedy R. Flow-injection analysis of hydrogen peroxide using a horseradish peroxidese — modified electrode detection system. Electroanalysis 1990;2:303–8.
[17] Santos AS, Pereira AC, Durán N, Kubota LT. Amperometric biosensor for ethanol based on co-immobilization of alcohol dehydrogenase and Meldola's Blue on multi-wall carbon nanotube. Electrochim Acta 2006;52:215–20.
[18] Ramirez Molina C, Boujtita M, El Murr N. A carbon paste electrode modified by entrapped toluidine blue-O for amperometric determination of L-lactate. Anal Chim Acta 1999;401:155–62.
[19] Ruan CM, Yang R, Chen XH, Deng JQ. A reagentless amperometric hydrogen peroxide biosensor based on covalently binding horseradish peroxidase and thionine using a thiol-modified gold electrode. J Electroanal Chem 1998;455:121–5.
[20] Guo Z, Shen Y, Wang M, Zhao F, Dong S. Anal. Electrochemistry and electrogenerated chemiluminescence of SiO_2 nanoparticles/tris(2,2'-bipyridyl) ruthenium (II) multilayer films on Indium Tin Oxide electrodes. Anal Chem 2004;76:184–91.
[21] Choi HN, Cho SH, Lee WY. Electrogenerated chemiluminescence from tris(2,2'-bipyridyl)ruthenium(II) immobilized in titania-perfluorosulfonated ionomer composite films. Anal Chem 2003;75:4250–6.
[22] Guo SJ, Wang EK. A novel sensitive solid-state electrochemiluminescence sensor material: $Ru(bpy)_3^{2+}$ doped SiO_2@MWNTs coaxial nanocable. Electrochem Commun 2007;9:1252–7.
[23] Tsionsky M, Gun G, Glezer V, Lev O. Sol–gel-derived ceramic-carbon composite electrodes: introduction and scope of applications. Anal Chem 1994;66:1747–53.
[24] Abdullah J, Ahmad M, Heng LK, Karuppiah N, Sidek H. Stacked films immobilization of MBTH in nafion/sol–gel silicate and horseradish peroxidase in chitosan for the determination of phenolic compounds. Anal Bioanal Chem 2006;5:1285–92.
[25] Zhang LH, Xu ZA, Dong SJ. Electrogenerated chemiluminescence biosensor based on $Ru(bpy)_3^{2+}$ and dehydrogenase immobilized in sol–gel/chitosan/poly(sodium 4-styrene sulfonate) composite material. Anal Chim Acta 2006;575:52–6.

[26] Ravi Shankaran D, Uehera N, Kato T. Determination of hydrogen peroxide based on a metal dispersed sol–gel derived ceramic–graphite composite electrode. Anal Bioanal Chem 2002;374:412–5.
[27] Wang L, Wang E. A novel hydrogen peroxide sensor based on horseradish peroxidase immobilized on colloidal Au modified ITO electrode. Electrochem Commun 2004;6:225–9.
[28] Enustun BV, Turkevich JJ. Coagulation of colloidal gold. J Am Chem Soc 1963;85:3317–28.
[29] Garbar KC, Griffith FR, Hommer MB, Natan MJ. Preparation and characterization of Au colloid monolayers. Anal Chem 1995;67:735–43.
[30] Lei CX, Hu SQ, Shen GL, Sens, Actuat B, Yu RQ. Immobilization of horseradish peroxidase to a nano-Au monolayer modified chitosan-entrapped carbon paste electrode for the detection of hydrogen peroxide. Talanta 2003; 59: 981–988.
[31] Michael RA, Arlon JH. Synthesis and properties of chitosan-silica hybrid aerogels. J Non-cryst Solids 2001;85:123–7.
[32] Yang YM, Wang JW, Tan RX. Immobilization of glucose oxidase on chitosan–SiO_2 gel. Enzyme Microb Technol 2004;34:126–31.
[33] Wang BQ, Zhang JZ, Cheng GJ, Dong SJ. Amperometric enzyme electrode for the determination of hydrogen peroxide based on sol–gel/hydrogel composite film. Anal Chim Acta 2000;407:111–8.
[34] Miao Y, Tan SN. Amperometric hydrogen peroxide biosensor with silica sol–gel/chitosan film as immobilization matrix. Anal Chim Acta 2001;437:87–93.
[35] Xu Q, Mao C, Liu NN, Zhu JJ, Shen J. Immobilization of horseradish peroxidase on O-carboxymethylated chitosan/sol–gel matrix. React Funct Polym 2006;66:863–70.
[36] Tangkuaram T, Ponchio C, Kangkasomboon T, Katikawong P, Veerasai W. Design and development of a highly stable hydrogen peroxide biosensor on screen printed carbon electrode based on horseradish peroxidase bound with gold nanoparticles in the matrix of chitosan. Biosens Bioelectron 2007;22:2071–8.
[37] Kamin RA, Willson GS. Rotating ring-disk enzyme electrode for biocatalysis kinetic studies and characterization of the immobilized enzyme layer. Anal Chem 1980;52:1198–1105.